

Journal of Visualized Experiments

Fabrication and Implementation of a Reference-Free Traction Force Microscopy Platform

--Manuscript Draft--

Article Type:	Methods Article - JoVE Produced Video
Manuscript Number:	JoVE60383R2
Full Title:	Fabrication and Implementation of a Reference-Free Traction Force Microscopy Platform
Keywords:	Mechanotransduction, Two-Photon Laser Scanning Lithography, Photopatterning, Cell Generated Forces, Biomaterials, Particle Tracking, Hydrogel, PEG, Strain, Deformation, 3D Printing
Corresponding Author:	John Hundley Slater, Ph.D. University of Delaware Newark, DE UNITED STATES
Corresponding Author's Institution:	University of Delaware
Corresponding Author E-Mail:	jhslater@udel.edu
Order of Authors:	Omar A. Banda John Hundley Slater, Ph.D.
Additional Information:	
Question	Response
Please indicate whether this article will be Standard Access or Open Access.	Standard Access (US\$2,400)
Please indicate the city, state/province, and country where this article will be filmed . Please do not use abbreviations.	Newark, Delaware, USA

TITLE:

Fabrication and Implementation of a Reference-Free Traction Force Microscopy Platform

AUTHORS AND AFFILIATIONS:

Omar A. Banda¹, John H. Slater^{1,2,3}

¹Department of Biomedical Engineering, University of Delaware, Newark, DE, USA

²Department of Materials Science & Engineering, University of Delaware, Newark, DE, USA

³Delaware Biotechnology Institute, Newark, DE, USA

Email addresses of co-authors:

Omar A. Banda (obanda@udel.edu)

Corresponding author:

John H. Slater (jhslater@udel.edu)

KEYWORDS:

mechanotransduction, two-photon laser scanning lithography, photopatterning, cell generated forces, biomaterials, particle tracking, hydrogel, PEG, strain, deformation, 3D printing

SUMMARY:

This protocol provides instructions for implementing multiphoton lithography to fabricate three-dimensional arrays of fluorescent fiducial markers embedded in poly(ethylene glycol)-based hydrogels for use as reference-free, traction force microscopy platforms. Using these instructions, measurement of 3D material strain and calculation of cellular tractions is simplified to promote high-throughput traction force measurements.

ABSTRACT:

Quantifying cell-induced material deformation provides useful information concerning how cells sense and respond to the physical properties of their microenvironment. While many approaches exist for measuring cell-induced material strain, here we provide a methodology for monitoring strain with sub-micron resolution in a reference-free manner. Using a two-photon activated photolithographic patterning process, we demonstrate how to generate mechanically and bio-actively tunable synthetic substrates containing embedded arrays of fluorescent fiducial markers to easily measure three-dimensional (3D) material deformation profiles in response to surface tractions. Using these substrates, cell tension profiles can be mapped using a single 3D image stack of a cell of interest. Our goal with this methodology is to make traction force microscopy a more accessible and easier to implement tool for researchers studying cellular mechanotransduction processes, especially newcomers to the field.

INTRODUCTION:

Traction force microscopy (TFM) is the process of approximating cellular tractions using interpolated displacement fields of fiducial markers generated by an adherent and contractile cell. Using TFM, the influence of mechanical cues in the extracellular environment on important cellular processes such as proliferation, differentiation, and migration can be investigated¹⁻¹².

Unfortunately, many existing approaches can be difficult to implement or require familiarity with highly specialized analytical and computational tools making TFM difficult for inexperienced researchers to use. We describe a methodology to generate a TFM platform that eliminates some of the difficulty in analysis while also providing high-throughput data acquisition.

Of the existing TFM approaches, the most commonly used for quantifying material strain involves incorporation of small fluorescent markers (typically nano- or micrometer-sized fluorescent beads) into a deformable hydrogel, such as polyacrylamide (PAA) or poly(ethylene glycol) diacrylate (PEGDA)^{13–15}. These bead-based approaches provide the ability to densely cluster fiducial markers around a cell of interest to maximize displacement sampling. Unfortunately, the distribution of the beads throughout the hydrogel cannot be directly controlled so the spatial organization is random. This random placement leads to problems such as beads which are too close to each other to accurately resolve, or so spread that patches of the substrate yield low quality data. The inability to predict where fiducial markers lie in the absence of cells also creates a constraint that, for every collected set of cell traction data, an additional reference image of the underlying markers in a relaxed state must also be captured. The reference image is required so that displacement in the stressed image can be approximated as the difference between the stressed and unstressed images. To achieve a relaxed state, the cells being measured are either chemically relaxed or completely removed. This process often prevents acquisition of further experimental measurements, inhibits long-term cell studies, and limits throughput. A reference image also requires image registration techniques to accommodate for drift which may have occurred during experimentation, often leading to cumbersome manual matching of stress state images to reference images.

Other TFM methods deemed reference-free, implement some form of control over the distribution of fiducial markers, either by high resolution lithography, microcontact printing, or micromolding^{16–20}. Reference-free TFM is achieved through the assumption that the relaxed state for each fiducial marker can be predicted based on how marker positions were prescribed during the fabrication process. These methods allow for complete capture of a cell's tension state within a single image capture in which fiducial marker displacements are measured in comparison to an implied reference than can be inferred from the fiducial marker geometry. While consistency in marker placement is typically achieved using these platforms, they generally suffer from their own shortcomings relative to the widely used bead-based approaches including: 1) decreased traction resolution; 2) decreased accuracy of out-of-plane displacements (in some cases a complete inability to measure); and 3) decreased customizability of platform substrates and materials (e.g., ligand presentation, mechanical properties).

To address these shortcomings, we designed a new reference-free TFM platform. The platform utilizes multiphoton activated chemistry to crosslink a small volume of a fluorophore into specific 3D locations within the hydrogel that serve as fiducial markers to measure material strain. In this way, we have designed a platform that operates similarly to bead-based approaches but with the significant benefit that fiducial markers are organized into gridded arrays allowing for reference-free material strain tracking. This reference-free property affords many advantages. First and foremost, it allows for non-intrusive monitoring of cellular traction states (i.e., circumvents the

need to relax or remove cells to acquire reference positions of displaced fiducial markers). This was our primary goal in designing this system, as we intended to incorporate other downstream analytical methods in tandem with TFM, which can be difficult with destructive end-point TFM approaches. Second, using an implied reference based on gridded arrays allows for near-complete automation of displacement analysis. The regularity of the arrays creates a predictable workflow where the occurrence of exceptional cases (i.e., sample cell data containing unanticipated artifacts such as suboptimal marker spacing or registration mismatches) can be maintained at a minimum. Third, forgoing the need to acquire a reference image provides the freedom to monitor many cells on a single sample over extended periods of time. This contrasts with traditional bead-based approaches, where, depending on the fidelity of the microscope's automated stage movements, errors in positioning can accumulate and increase the difficulty of properly registering reference images to cell tension images. Overall, this platform facilitates higher throughput in collecting cellular tension data.

With this protocol, we hope to familiarize the readers with the two-photon, laser scanning lithography technique that we implemented to generate this reference-free TFM platform to measure in-plane and out-of-plane traction components generated by cells seeded on the surface. Not covered in this protocol is the synthesis of some of the monomeric components. In general, these reactions include nearly identical "one-pot" synthesis reaction schemes described previously²¹, and alternatives to these products can also be purchased. We also aim to familiarize readers with the software-based tools we generated to promote the use of commercially-available laser-scanning microscopes as 3D printing tools and to facilitate analysis of fiducial marker displacements.

PROTOCOL:

1. Photopolymerizing a PEGDA base hydrogel

1.1 Gathering Reagents

1.1.1 Collect lithium phenyl-2,4,6-trimethylbenzoylphosphinate (LAP), 3.4 kDa poly(ethylene) glycol diacrylate (PEGDA), n-vinyl pyrrolidone (NVP), AlexaFluor 488 labeled PEGDA (PEG-488), AlexaFluor 633 labeled PEGDA (PEG-633), and PEGylated RGDS peptide (PEG-RGDS) from their respective freezers and bring each to room temperature.

1.1.2 In separate amber microcentrifuge tubes, measure 3 mg of LAP, 10 mg of PEGDA, 5 mg of PEG-488, 20 mg of PEG-633, and 6 mg of RGDS peptide.

1.2 Preparation of the Pre-Polymer Solution

1.2.1 Dissolve the LAP in 1 mL of phosphate buffered saline (PBS, pH 7.4). Use 200 μ L of the dissolved LAP solution to dissolve the PEGDA. Then, use 200 μ L of the PEGDA solution to dissolve the PEG-RGDS.

NOTE: If control of cell shape is desired, omit dissolving PEG-RGDS in the base hydrogel pre-polymer solution, as it will be added via two-photon, laser scanning lithography later in the protocol.

1.2.2 Use 80 μL of PBS to dissolve the PEG-488. Add 2.5 μL of this solution to the pre-polymer solution.

NOTE: The PEG-488 will give the final hydrogel a fluorescent signal which can be used to navigate during patterning and the concentration can be modified to alter the signal intensity.

1.2.3 Filter the complete pre-polymer solution through a 0.2 μm polytetrafluoroethylene (PTFE) filter to remove any particulates that may be present in the solution. If reactants are properly synthesized, the filter should not become clogged.

1.3 Photopolymerizing the base hydrogel

1.3.1 Place 3 μL of the pre-polymer solution on a thin flat sheet of perfluoroalkoxy alkanes (PFA). Place flat 150 μm thick polydimethylsiloxane (PDMS) strips surrounding, but not in contact with, the drop of pre-polymer solution. Place an acrylate-silanized coverslip²¹⁻²⁴ on the PDMS—with the pre-polymer droplet centered under the coverslip—to flatten the pre-polymer droplet to the thickness of the PDMS spacers.

1.3.2 Expose the sandwiched pre-polymer solution to UV light until a hydrogel is fully formed (approximately 1 min at 14 mW/cm^2 of 370-400nm light).

1.3.3 Carefully separate the coverslip from the PDMS spacers and attach to an open-bottom Petri dish using high-performance, double-sided acrylic adhesive. Apply pressure to the adhesive contact surface to create a complete seal between the coverslip, adhesive, and Petri dish—with care not to crack the glass.

1.3.4 Rinse the hydrogel in the Petri dish using sterile-filtered PBS to minimize biological and particulate contaminants.

1.3.5 Repeat steps 1.3.1-1.3.4 as needed to create the desired number of hydrogels.

1.3.6 Add 8 μL of NVP to the remaining 800 μL of LAP solution and keep this solution as well as undissolved PEG-633 until ready to pattern.

NOTE: The LAP solution with NVP is very sensitive to light and will polymerize if not kept in the dark. Wrapping the tube in aluminum foil can help improve its shelf life.

2. Creating patterning instructions

2.1 Designing a binary image

2.1.1 To create a virtual mask for prescribing fiducial marker arrays, use image-processing or drawing software to create an image with an aspect ratio of 100:1 (e.g., 2000 pixels long x 20 pixels wide).

2.1.2 Create a row of 100 evenly spaced white pixels on a black background centered along the long axis of the image.

2.1.3 Save this image as a *.tif filetype.

NOTE: If control of cell shape is desired^{21, 25–28}, create an additional virtual mask. Use a square shaped image canvas and create positive white features on a black background. For approximating an appropriate size for the white features (which will eventually support cell adhesion) assume that the total size of the image is equivalent to the size of the microscope's viewfield used for laser scanning lithography.

2.2 Converting a binary image to a digital mask

2.2.1 Download the LSM-ROI-Generator functions available free at the software repository²⁹.

2.2.2 Open Matlab and find the directory of the downloaded function files. Once in the directory, open the **run_script.m** Matlab script and run the script.

2.2.3 Select the binary *.tif file for conversion. Then, select a folder to save regions files.

2.2.4 Input the desired final size, in microns, of the selected image. The input image will be scaled and dimensioned to match these parameters. For the entire image to fit in the viewfield of the microscope, the total size of the image must be less than or equal to the size of the microscope viewfield.

2.2.5 If creating a single pixel array, in the ROI-Generator Options, make sure to uncheck the **Remove** tickbox under **Small Regions/Single Pixels**, to check the tickbox labeled **Squares**, and to uncheck **Use** under **Horizontal Break Lines**. Then, click **OK**.

NOTE: If creating a regions file to create single cell patterns the default options are appropriate.

2.2.6 Find the resulting *.ovl file in the previously specified folder. This file must be brought to the microscope to load the desired regions that control the laser shutter during two-photon laser scanning lithography.

3 Fabricating fiducial marker arrays

3.1 Soaking the base hydrogel

3.1.1 Under low light conditions, add 200 μ L of the LAP/NVP solution to the AF633 (both prepared in step 1). Mix thoroughly while protecting from light.

3.1.2 Remove all PBS solution from the Petri dish containing a PEGDA hydrogel from step 1.

3.1.3 Add the dissolved PEG-633 to the hydrogel to form a droplet that completely encompasses the base hydrogel.

NOTE: If the hole in the Petri dish is only slightly larger than the hydrogel, it can serve as a well to hold the patterning solution. Otherwise, make sure that the coverslip is completely dry before adding patterning solution or it may run off the hydrogel causing the hydrogel to dehydrate during patterning.

3.1.4 Load the Petri dish onto the sample holder on the microscope stage and place the lid on the Petri dish. Allow the patterning solution to soak into the hydrogel for at least 30 min in the dark.

NOTE: The microscope can be turned on and configured during this soak time. Using the 488 nm laser to image the hydrogel during soaking is fine.

3.2 Configuring the microscope

3.2.1 Using a 488 nm laser line and filters appropriate to image AlexaFluor 488, locate the hydrogel using the PEG-488 signal. Block collection of longer emission wavelengths from the detector as these will be saturated with signal from the PEG-633.

3.2.2 Find the center of the hydrogel in the XY plane using vertical and horizontal tile scans and zero the stage position here.

3.2.3 Find the surface of the hydrogel using line scans and the z-stack function. Zero the focus position here. Level the hydrogel by repeating these line scans away from the XY center to identify the surface position and adjusting the set screws for the microscope stage.

3.2.4 Within the microscope software workspace, create a separate experiment file for photopatterning. Set the multiphoton power to 1.8% (15.5 mW at 740 nm as measured at the back aperture of the objective), and the scanning speed to 6 (0.1 μ m/ μ s). Adjust the size of the image frame in pixels to achieve a pixel size of 0.1 μ m per pixel and an aspect ratio of 100:1.

3.2.5 Load the regions file (*.ovl) created in step 2.2 into the regions tab. Use a macro to set all regions to acquisition.

3.2.6 Turn on the z-stack function and set the spacing to 3.5 μ m for a total depth of 28 μ m and total number of z-slices of 9.

3.2.7 Use the positions function to set specific locations on the hydrogel where the fiducial marker arrays will be photopatterned.

NOTE: The z-location of these positions will dictate the center position of each z-stack; when placing positions, be sure that each position will guarantee that the patterned volume will overlap with the hydrogel at all surface locations.

3.2.8 Use the tile function to specify additional rows and columns at each position. Be careful to avoid overlapping patterned regions. Ideally, make sure that patterned areas are close enough to remove empty and unusable locations between positions.

3.3 Photopatterning the fiducial marker arrays

3.3.1 As soak time approaches the 30 min mark, take successive z-stack line scans of the surface of the hydrogel every 5 min to check for swelling based on changes in the location of surface relative to the zeroed focus position.

3.3.2 If no change in the surface position occurs over a 5 min interval, load and run the patterning settings created in step 3.2.4

3.3.3 Once the patterning experiment has finished running, use the 488 nm laser to verify that the surface of the hydrogel did not move during patterning.

NOTE: If the surface of the hydrogel is not in the same position as it was prior to patterning, several scenarios exist. The hydrogel had not reached swelling equilibrium prior to patterning, the hydrogel began to dry out during patterning, or the microscope experienced z-drift. The source of this surface translation should be identified and corrected in subsequent patterning runs.

3.3.4 Remove the hydrogel from the microscope and aspirate the PEG-633 solution from the Petri dish.

NOTE: The hydrogel is still extremely sensitive to light. Keeping the hydrogel in the dark is very important until all rinsing is complete.

3.3.5 Rinse the hydrogel 3 times with sterile-filtered PBS, making sure to completely remove rinsate between each successive rinse. Repeat this triple rinse every 15 min for 1 h.

3.3.6 Allow the hydrogel to rinse in PBS overnight.

NOTE: The protocol can be paused here.

3.3.7 Triple rinse the hydrogel with PBS. Then quickly triple rinse the hydrogel with a 200-proof ethanol solution, followed by another triple rinse with PBS. Do not allow the hydrogel to sit in 200 proof ethanol for extended periods of time.

NOTE: Some components of the patterning solution can crash out of solution and deposit onto the surface of the hydrogel and appear as a solid layer of fluorescence (~1-5 microns thick) under 633 nm illumination. Rinsing with 200 proof ethanol should remove these unwanted components.

3.4 Using successive photopatterning to generate single cell patterns (Optional)

NOTE: If control over cell spread area and shape is desired, multiple rounds of patterning can be performed. The base gel must have PEG-RGDS omitted from its initial formulation. It is recommended that patterning of the fiducial marker arrays be performed last to avoid bleaching of the fluorescent fiducial markers.

3.4.1 Dissolve 20 mg of PEG-RGDS in the LAP/NVP solution prepared in step 1.

3.4.2 Repeat steps 3.1 – 3.3 using the PEG-RGDS solution instead of the PEG-633 solution. Use the appropriate regions file that defines the single cell patterns (see step 2 for instructions)

NOTE: To visualize the arrays of PEG-RGDS patterns, there are several options. A fluorescent variant of PEG-RGDS can be used^{21, 30} or the PEG-RGDS can be doped with fluorescent PEG. Recommended: Alternatively, the 488 nm laser line can be run in tandem with the multiphoton patterning laser to bleach PEG-488 signal in the base hydrogel, creating non-fluorescent regions that coincide with RGDS incorporation.

4 Visualizing fiducial marker arrays

4.1 Acquiring a z-stack image of the fabricated array

4.1.1 Replace PBS in the Petri dish with the cell media used for cell culture.

NOTE: Phenol red free media is recommended for use during image acquisition to prevent phototoxicity.

4.1.2 After 1 h of soak time, use a widefield fluorescence microscope equipped with a structured illumination module and a high-magnification water immersion objective lens to visualize the hydrogels using a filter set appropriate for the fluorescent fiducial markers.

4.1.3 Collect a high-resolution z-stack of images (spaced 0.4 μm in Z) encompassing at least 20 μm of depth from the surface of the hydrogel into the hydrogel in the patterned area, making sure the upper limit of the z-stack includes at least 1-2 images physically above the patterned area (i.e., where the fluorescent fiducial markers are no longer visible and only noise is present).

NOTE: Acquisition of this image stack is necessary to verify that all patterning parameters are correct and can be analyzed alongside cell data in step 5.3.

5 Performing TFM using photopatterned hydrogels

5.1 Seeding Cells

NOTE: To maintain sterility, follow all standard tissue culture practices.

5.1.1 Prior to cell seeding, follow standard protocols for the respective cell line for cell culture and maintenance.

5.1.2 (Optional) If sterility of the hydrogel is a concern, incubate the hydrogel for 24 h in media containing antibiotics followed by rinsing with normal media.

5.1.3 To seed cells, first re-suspend trypsinized cells in the final volume of media to be used in the hydrogel Petri dish.

5.1.4 Remove all solution from the hydrogel dish and replace with the cell-laden media.

5.1.5 Allow the hydrogel to sit undisturbed in cell-laden media for 10 min.

5.1.6 Carefully move the Petri dish to an incubator. Maintain the cells in the incubator for 4 h or until the cells are visibly adhered.

5.1.7 Replace the cell-laden media with cell-free media to remove unadhered cells.

5.2 Acquiring images of cells and the fiducial markers

5.2.1 Set the temperature for the incubation chamber on the microscope to 37 °C and CO₂ to 5% and allow the chamber to reach the set points.

5.2.2 Place the Petri dish on the sample holder and locate the patterned areas.

5.2.3 Locate a cell of interest (COI) and acquire a transmitted or fluorescent image of the COI.

NOTE: This image will be used to segment the cell boundary during analysis, so the image should clearly visualize the cell borders.

5.2.4 Acquire a z-stack of the patterned array beneath the COI as in step 4.1.4.

5.2.5 Acquire a second set of transmitted or fluorescent images of the cell.

NOTE: Compare the second image set to the first to determine if cell damage due to phototoxicity is observed and whether the image acquisition settings need to be adjusted. Cells which shrink after exposure have likely suffered significant phototoxic effects, which may affect results.

5.2.6 Repeat steps 5.2.3-5.2.5 for each COI.

6 Analyzing the Images

6.1 Preparation of the image files for analysis

6.1.1 Using data collected in step 5.2, prepare a cropped image stack of the area around a COI such that the bottom image (first image) of the stack represents the first frame where: (1) >80% of the patterned marker columns are visible, (2) the uppermost image (last image) in the stack no longer contains any visible fiducial markers (i.e., above the hydrogel surface), and (3) there is at least 20 μm of non-stressed fiducial markers surrounding the COI.

NOTE: Cropping the images greatly reduces computational time during analysis. The analysis code in later steps can be run without cropping the images but this is not recommended.

6.1.2 Create a cropped image of the transmitted and/or fluorescent image to match the XY cropping of the stack in the previous step.

6.1.3 Use either the cropped transmitted or fluorescent image—whichever is more representative of the cell shape—to segment the image by hand (trace the cell border) or via image processing tools.

6.1.4 Convert this image into a binary image where the interior of the cell is black (i.e., intensity = 0) and the area surrounding the cell is white (i.e., intensity \neq 0). Save this image as **Binary Mask.tif**.

6.1.5 For each COI, collect the image stack file, transmitted image file, and binary mask file in a single folder.

6.2 Running analysis scripts on the images

6.2.1 Clone or download the TFM analysis functions available free at the software repository²⁹. The entire repository should be downloaded as there are a significant number of dependencies in the subfolders.

6.2.2 Open Matlab and add the directory and all subfolders of the local clone of the code repository to the path.

6.2.3 Set the directory within the Matlab workspace to the folder location where the prepared images in step 6.1 were stored.

6.2.4 Open and run the **tracking.m** script. When prompted, follow the instructions to load the appropriate images, perform initial pre-processing steps, and error-check the object tracking algorithm.

6.2.5 Once the script has completed, open and run the **dispShear.m** function. This script should not require input from the user.

6.2.6 Once the **dispShear.m** script has completed, open and run **disp3D.m**. If prompted to open any images, follow the instructions.

NOTE: During runtime, the script may ask the user to draw a line on an image of the patterned array. This line should represent the primary motion axis of the scanning laser during patterning and should line-up with a row of patterned fiducial markers. This process instructs the code as to which direction (i.e., rows or columns of fiducial markers) likely yields the most aligned rows of fiducial markers.

6.2.7 Once the **dispShear.m** code has completed, run the **dispSurface.m** code followed by the **interpFinal3D_2.m** code. These scripts should not require inputs from the user.

NOTE: The **interpFinal3D_2.m** script converts displacement data into surface tractions using software obtained externally, which has been previously described³¹. To apply these external functions, the **interpFinal3D_2.m** interpolates displacement data into uniform grids to serve as inputs for the conversion functions. If using a different conversion method, or if tractions are not needed, this step can be skipped.

6.2.8 Once all scripts have been run, ensure all data and outputs can be found in the initial directory.

6.2.9 Repeat steps 6.2.3 – 6.2.8 for each COI.

NOTE: Within the code repository, there is a folder containing scripts that allow automatic batch running of each of the scripts on a list of directories. Refer to the automation scripts themselves (i.e., comments within the code) for instructions on how to use them.

REPRESENTATIVE RESULTS:

Throughout the protocol, there are a number of checkpoints providing feedback to assess the quality of the patterning procedure. To provide some insight concerning how to assess progress at each of these checkpoints, we provide representative results of an actual experiment. The results highlight the application of this protocol performed on a photopatterned hydrogel prepared for TFM analysis of human umbilical vein endothelial cells (HUVECs). The results include raw image data as well as processed data outputs at each critical step.

The first checkpoint occurs at step 4, once the fiducial marker array has been photopatterned in

the hydrogel. When collecting an image stack, the resulting images should display a regular array of patterned features (**Figure 1A-C**) that oscillate in intensity as a function of z-position within the image stack. If the patterned surface was not perfectly level, different regions of each image slice may seem out of phase with each other with respect to these oscillations; this is expected and should not affect analysis except in extreme cases.

The remaining checkpoints utilize outputs from each of the scripts run during analysis of a given COI. The **tracking.m** script provides several diagnostic images including a z-projection of fluorescent fiducial markers (**Figure 2A**) to assess pre-processing quality, a plot of detected centroids color coded as a function of z-position (**Figure 2B**) to assess object detection quality, and a plot of tracks representing detected marker centroids which have been linked into columns in the z-direction (**Figure 2C**) to assess object tracking quality.

For accurate 3D centroid detection necessary to calculate reference coordinates and displacements, fluorescent fiducial markers should resemble ellipsoidal shapes with intensity decreasing radially from the center. The **disp3D.m** script provides a plot of intensity as a function of z-position for each column of detected features in a given image stack (**Figure 3A,B**) to assess the quality of the fiducial marker intensity profiles. Both **disp3D.m** and **dispShear.m** together provide histograms of measured displacement noise in each of the Cartesian coordinate dimensions (**Figure 4A-C**) as well as interpolated heat maps of displacement (**Figure 4E,F**). Finally, the **interpFinal3D_2.m** provides heat maps of surface tractions calculated using outsourced code (**Figure 5**)³¹.

FIGURE AND TABLE LEGENDS:

Figure 1: Typical patterning results. (A) Fluorescent images of fiducial markers displaying intensity fluctuations through the Z-dimension from the hydrogel surface to 12.4 μm within the hydrogel. (B) A processed volumetric rendering reveals the ellipsoidal shape of the fiducial markers. (C) Sectioned profile views of the volumetric rendering display raw marker data. A,C: Scale bar = 5 μm .

Figure 2: Diagnostic outputs from the particle tracking algorithm. The object detection and tracking software outputs several diagnostic images including (A) a Z-weighted projection of the fluorescent fiducial markers and (B) a scatter plot of marker positions with color coded Z-position. (C) An additional output displays a z-weighted projection, as in (A), with 2D detections from each frame linked into columns. (D) A closer look at (B) more clearly shows individual 2D detections color coded by z-position. A: Scale bar = 20 μm . C: Scale bar = 5 μm .

Figure 3: Diagnostic outputs from the 3D displacement algorithm. (A, B) Line plots of marker intensity as a function of frame position display oscillations between markers grouped in the vertical direction. These line plots allow for qualitative assessment of grid alignment with the imaging plane, as well as overall quality of the patterned fiducial markers. (A) Overlapping oscillations in marker intensity confirm acceptable alignment of the imaging plane with the patterned fiducial marker arrays. Including empty frames at the top of a Z-stack allows for automated calculation of a noise threshold in the processing software. (B) Poor overlap between

oscillations is often indicative of poor alignment of the patterned grids with the imaging plane but may also suggest that the grid themselves are misaligned and may yield poor results.

Figure 4: Diagnostic outputs from the 2D and 3D displacement algorithms. (A-C) Histograms of measured displacements in regions considered 'non-deformed' (i.e., displacement noise) provide a quantitative assessment of the accuracy of calculated reference lines for approximating marker reference positions. Displacement fields provide a visual representation of both (D) in-plane (shear) and (E) out-of-plane (normal) measured displacements. D: Scale bar = 20 μm .

Figure 5: Diagnostic Outputs from the Traction Conversion Algorithm. (A-C) Traction stresses can be calculated based on interpolated displacement fields to determine the (B) total traction, (C) shear traction, and (D) normal traction. A: Scale bar = 20 μm .

DISCUSSION:

The goal of this protocol is to provide a workflow that alleviates much of the difficulty associated with the generation and analysis of TFM data. Once prepared, the photopatterned hydrogels are simple to use, requiring only knowledge of standard tissue culture practices and fluorescence microscopy. The reference-free aspect enables carefree navigation on cell-laden hydrogels and eliminates cumbersome image processing steps such as image registration between reference and deformed images. The resulting analysis is nearly completely automated and data from individual COIs can be analyzed from start to finish in less than 10 min.

The primary challenges in this protocol stem from the fabrication of the photopatterned hydrogel. Because most of the reagents used in the protocol are synthesized in-house, we expect that users with little experience using synthetic hydrogel materials may be somewhat deterred from attempting this protocol. That said, all of the PEGylated components used in this protocol are synthesized from nearly identical protocols using one-pot reactions and many of the components can be purchased from commercial vendors.

This protocol also requires some mastery over the use of laser-scanning microscopes. The laser-scanning parameters need to be optimized for every different microscope, as laser intensities, objective lenses, and other microscope components will vary, even between microscopes of the same model. A simple approach to determining the best microscope settings for photopatterning is to perform a panel of scans with varied settings. Any setting that affects the total laser exposure received by the sample will affect the size and quality of the patterned markers. This includes: scan speed, pixel size, averaging number, laser power/intensity/fluence, magnification, and numerical aperture^{32, 33}. It is often easiest to adjust laser power and scan speed and so it is recommended to start with those two parameters. It should also be noted that the software used to generate regions files was designed specifically for the brand of microscopes we use and may need to be augmented to accommodate other microscope makes and models. With the settings provided in the protocol, the user should expect to generate ellipsoidal markers with 3D gaussian-like intensity profiles of full-width half-max dimensions of $0.84 \pm 0.11 \mu\text{m}$ in XY and $3.73 \pm 0.30 \mu\text{m}$ in Z. The object detection algorithm uses a center-of-mass of intensity to identify marker centroids and will perform best when markers present a definite gradient of

intensity.

Properly rinsing the hydrogel and protecting it from light and from contaminants is critically important for cell culture. As mentioned in the protocol, some of the patterning components may crash out of solution and deposit on the surface of the hydrogel. If these components are not completely rinsed from the surface, cell adhesion may be unpredictably affected. If exposed to UV spectrum light, even in small doses, while the hydrogel is soaking in the patterning solution, the patterning solution will begin to polymerize and will yield poor results. Finally, airborne particulates or unfiltered particulates will complicate analysis, especially if they are fluorescent. Special care should be taken to prevent these contaminants from entering the sample at all steps in the protocol.

The analysis code predicts reference locations of deformed fiducial markers by predicting the original array from non-deformed markers in the same row or column as the deformed marker. While this greatly simplifies analysis, it also imposes some restrictions on what can or cannot be analyzed. At a minimum, each deformed marker being analyzed should have 2 or more members of both its column and row of markers which are not deformed so that an accurate prediction can be made. A row is defined by the group of dots printed in a single line scan on the microscope, and a column is defined by markers patterned on a single vertical axis using a z-stack function. This limits analysis to single cells or small cell clusters based on the length and depth of each patterned area. It is important to note that this is not remedied by placing two patterned regions perfectly next to each other. This is because although the XY components may line up, it is not feasible to perfectly line up the Z positional components of the arrays, unless the sample surface is perfectly level with both the focal plane and the stage. The best way to avoid this limitation is to employ additional rounds of patterning that specifically dictate adhesion ligand placement. If aligned properly, cell adhesion can be restricted to usable areas on the patterns.

The analysis code has been optimized for square arrays where markers are spaced approximately 3.5 μm apart in Z and 2.1 μm in X and Y. The final spacing will vary based on patterning fidelity and swelling, but this should not greatly impact performance if in-row spacing is consistent (inter-row spacing variability will not affect tracking). While the code may run to completion on differently prescribed arrays, its current state may yield poor results if the arrays do not match the parameters listed here. Our current goals for the analysis code are to include support for variable spacing as well as triangular arrays, which may improve traction reconstruction accuracy and reduce regional bias as compared to square arrays.

To conclude, we provide an approach to TFM that allows for facile collection and analysis of TFM data without perturbing cellular function. Our goal with this approach is to provide a more accessible and non-intrusive TFM approach, without compromising the resolution and quality of TFM data. We expect that this methodology will promote the convergence of biochemical knowledge of cellular phenotypes with the observed physical properties of cells.

ACKNOWLEDGMENTS:

O. A. Banda was supported by funding from a NSF IGERT SBE2 fellowship (1144726), startup funds

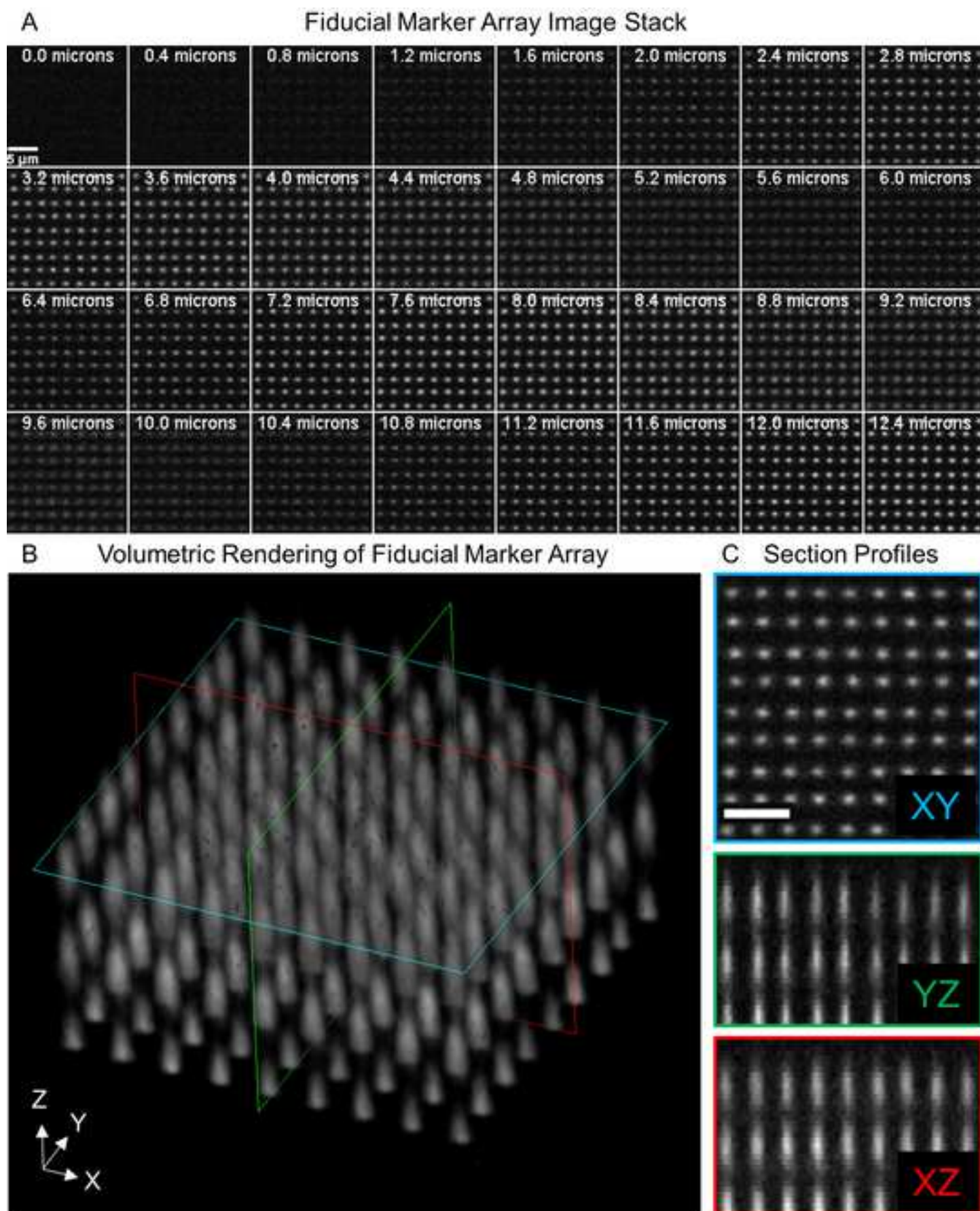
provided by the University of Delaware, and the National Institutes of Health/National Cancer Institute IMAT Program (R21CA214299). JHS is supported by funding from the National Institutes of Health/National Cancer Institute IMAT Program (R21CA214299) and the National Science Foundation CAREER Award Program (1751797). Microscopy access was supported by grants from the NIH-NIGMS (P20 GM103446), the NSF (IIA-1301765) and the State of Delaware. The structured illumination microscope was acquired with funds from the State of Delaware Federal Research and Development Grant Program (16A00471). The LSM880 confocal microscope used for two-photon laser scanning lithography was acquired with a shared instrumentation grant (S10 OD016361).

REFERENCES:

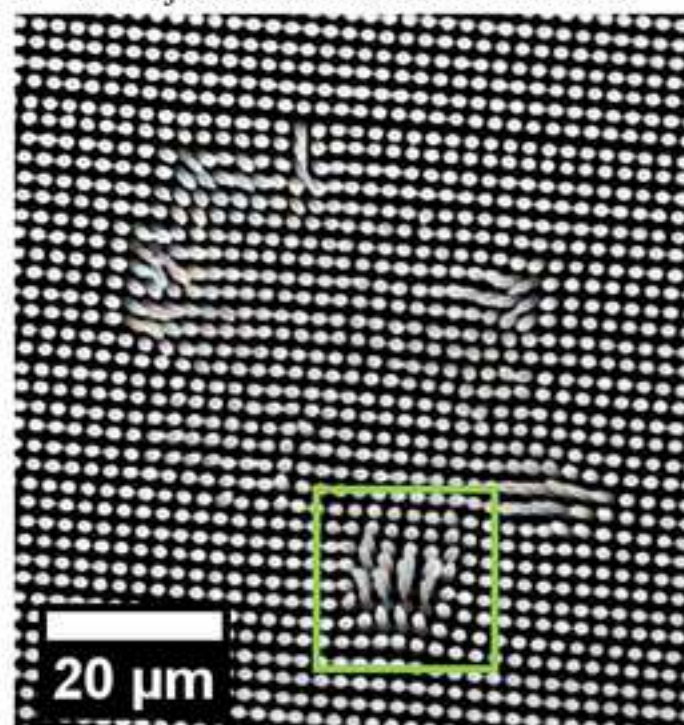
1. Rauskolb, C., Sun, S., Sun, G., Pan, Y., Irvine, K.D. Cytoskeletal tension inhibits Hippo signaling through an Ajuba-Warts complex. *Cell*. **158** (1), 143–156, doi: 10.1016/j.cell.2014.05.035 (2014).
2. Huang, S., Chen, C.S., Ingber, D.E. Control of Cyclin D1, p27Kip1, and Cell Cycle Progression in Human Capillary Endothelial Cells by Cell Shape and Cytoskeletal Tension. *Molecular Biology of the Cell*. **9** (11), 3179–3193, doi: 10.1091/mbc.9.11.3179 (1998).
3. Plotnikov, S. V., Pasapera, A.M., Sabass, B., Waterman, C.M. Force Fluctuations within Focal Adhesions Mediate ECM-Rigidity Sensing to Guide Directed Cell Migration. *Cell*. **151** (7), 1513–1527, doi: 10.1016/j.cell.2012.11.034 (2012).
4. Álvarez-González, B., Meili, R., Bastounis, E., Firtel, R.A., Lasheras, J.C., Del Álamo, J.C. Three-dimensional balance of cortical tension and axial contractility enables fast amoeboid migration. *Biophysical Journal*. **108** (4), 821–832, doi: 10.1016/j.bpj.2014.11.3478 (2015).
5. Provenzano, P.P., Keely, P.J. Mechanical signaling through the cytoskeleton regulates cell proliferation by coordinated focal adhesion and Rho GTPase signaling. *Journal of Cell Science*. **124** (8), 1195–1205, doi: 10.1242/jcs.067009 (2011).
6. Reilly, G.C., Engler, A.J. Intrinsic extracellular matrix properties regulate stem cell differentiation. *Journal of Biomechanics*. **43** (1), 55–62, doi: 10.1016/j.jbiomech.2009.09.009 (2010).
7. Wen, J.H. *et al.* Interplay of matrix stiffness and protein tethering in stem cell differentiation. *Nature Materials*. **13** (10), 979–987, doi: 10.1038/nmat4051 (2014).
8. Lee, J., Abdeen, A.A., Tang, X., Saif, T.A., Kilian, K.A. Geometric guidance of integrin mediated traction stress during stem cell differentiation. *Biomaterials*. **69**, 174–183, doi: 10.1016/j.biomaterials.2015.08.005 (2015).
9. Steward, A.J., Kelly, D.J. Mechanical regulation of mesenchymal stem cell differentiation. *Journal of Anatomy*. **227** (6), 717–731, doi: 10.1111/joa.12243 (2015).
10. Lv, H. *et al.* Mechanism of regulation of stem cell differentiation by matrix stiffness. *Stem Cell Research & Therapy*. **6** (1), 103, doi: 10.1186/s13287-015-0083-4 (2015).
11. Tijore, A. *et al.* Role of Cytoskeletal Tension in the Induction of Cardiomyogenic Differentiation in Micropatterned Human Mesenchymal Stem Cell. *Advanced Healthcare Materials*. **4** (9), 1399–1407, doi: 10.1002/adhm.201500196 (2015).
12. Lombardi, M.L., Knecht, D.A., Dembo, M., Lee, J. Traction force microscopy in Dictyostelium reveals distinct roles for myosin II motor and actin-crosslinking activity in polarized cell movement. *Journal of Cell Science*. **120** (9), 1624–1634, doi: 10.1242/jcs.002527 (2007).

13. Legant, W.R. *et al.* Multidimensional traction force microscopy reveals out-of-plane rotational moments about focal adhesions. *Proceedings of the National Academy of Sciences*. **110** (3), 881–886, doi: 10.1073/pnas.1207997110 (2013).
14. Sabass, B., Gardel, M.L., Waterman, C.M., Schwarz, U.S. High resolution traction force microscopy based on experimental and computational advances. *Biophysical Journal*. **94** (1), 207–220, doi: 10.1529/biophysj.107.113670 (2008).
15. Munevar, S., Wang, Y., Dembo, M. Traction Force Microscopy of Migrating Normal and H-ras Transformed 3T3 Fibroblasts. *Biophysical Journal*. **80** (4), 1744–1757, doi: 10.1016/S0006-3495(01)76145-0 (2001).
16. Pushkarsky, I. *et al.* Elastomeric sensor surfaces for high-Throughput single-cell force cytometry. *Nature Biomedical Engineering*. **2** (2), 124–137, doi: 10.1038/s41551-018-0193-2 (2018).
17. Bergert, M. *et al.* Confocal reference free traction force microscopy. *Nature Communications*. **7**, doi: 10.1038/ncomms12814 (2016).
18. Schwarz, U.S. *et al.* Measurement of cellular forces at focal adhesions using elastic micro-patterned substrates. *Materials Science and Engineering: C*. **23** (3), 387–394, doi: 10.1016/S0928-4931(02)00309-0 (2003).
19. Tan, J.L., Tien, J., Pirone, D.M., Gray, D.S., Bhadriraju, K., Chen, C.S. Cells lying on a bed of microneedles: An approach to isolate mechanical force. *Proceedings of the National Academy of Sciences*. **100** (4), 1484–1489, doi: 10.1073/pnas.0235407100 (2003).
20. Desai, R. a., Yang, M.T., Sniadecki, N.J., Legant, W.R., Chen, C.S. Microfabricated Post-Array-Detectors (mPADs): an Approach to Isolate Mechanical Forces. *Journal of Visualized Experiments*. (0), 1–5, doi: 10.3791/311 (2007).
21. Banda, O.A., Sabanayagam, C.R., Slater, J.H. Reference-Free Traction Force Microscopy Platform Fabricated via Two-Photon Laser Scanning Lithography Enables Facile Measurement of Cell-Generated Forces. *ACS Applied Materials & Interfaces*. **11** (20), 18233–18241, doi: 10.1021/acsami.9b04362 (2019).
22. Guo, J., Keller, K.A., Govyadinov, P., Ruchhoeft, P., Slater, J.H., Mayerich, D. Accurate flow in augmented networks (AFAN): an approach to generating three-dimensional biomimetic microfluidic networks with controlled flow. *Analytical Methods*. **11** (1), 8–16, doi: 10.1039/C8AY01798K (2019).
23. Heintz, K.A., Mayerich, D., Slater, J.H. Image-guided, Laser-based Fabrication of Vascular-derived Microfluidic Networks. *Journal of Visualized Experiments*. (119), 1–10, doi: 10.3791/55101 (2017).
24. Heintz, K.A., Bregenzer, M.E., Mantle, J.L., Lee, K.H., West, J.L., Slater, J.H. Fabrication of 3D Biomimetic Microfluidic Networks in Hydrogels. *Advanced Healthcare Materials*. **5** (17), 2153–2160, doi: 10.1002/adhm.201600351 (2016).
25. Slater, J.H., Miller, J.S., Yu, S.S., West, J.L. Fabrication of Multifaceted Micropatterned Surfaces with Laser Scanning Lithography. *Advanced Functional Materials*. **21** (15), 2876–2888, doi: 10.1002/adfm.201100297 (2011).
26. Slater, J.H. *et al.* Recapitulation and Modulation of the Cellular Architecture of a User-Chosen Cell of Interest Using Cell-Derived, Biomimetic Patterning. *ACS Nano*. **9** (6), 6128–6138, doi: 10.1021/acs.nano.5b01366 (2015).
27. Shukla, A., Slater, J.H., Culver, J.C., Dickinson, M.E., West, J.L. Biomimetic Surface

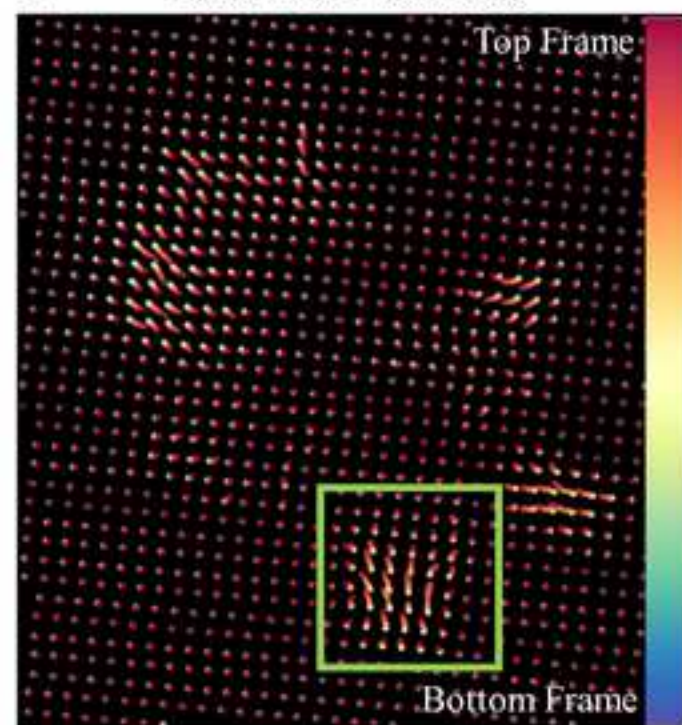
- Patterning Promotes Mesenchymal Stem Cell Differentiation. *ACS Applied Materials & Interfaces*. **8** (34), 21883–21892, doi: 10.1021/acsami.5b08978 (2016).
28. Slater, H.J., Banda, A.O., Heintz, A.K., Nie, T.H. Biomimetic Surfaces for Cell Engineering. *Carbon Nanomaterials for Biomedical Applications*. 543–569, doi: 10.1007/978-3-319-22861-7_18 (2016).
29. Banda, O.A., Slater, J.H. Slater Lab Code Repositories. at <<https://github.com/SlaterLab>> (2019).
30. Culver, J.C., Hoffmann, J.C., Poché, R.A., Slater, J.H., West, J.L., Dickinson, M.E. Three-dimensional biomimetic patterning in hydrogels to guide cellular organization. *Advanced Materials*. **24** (17), 2344–2348, doi: 10.1002/adma.201200395 (2012).
31. Toyjanova, J., Bar-Kochba, E., López-Fagundo, C., Reichner, J., Hoffman-Kim, D., Franck, C. High resolution, large deformation 3D traction force microscopy. *PLoS ONE*. **9** (4), 1–12, doi: 10.1371/journal.pone.0090976 (2014).
32. Pradhan, S., Keller, K.A., Sperduto, J.L., Slater, J.H. Fundamentals of Laser-Based Hydrogel Degradation and Applications in Cell and Tissue Engineering. *Advanced Healthcare Materials*. **6** (24), 1–28, doi: 10.1002/adhm.201700681 (2017).
33. Tibbitt, M.W., Shadish, J.A., DeForest, C.A. Photopolymers for Multiphoton Lithography in Biomaterials and Hydrogels. *Multiphoton Lithography*. 183–220, doi: 10.1002/9783527682676.ch8 (2016).



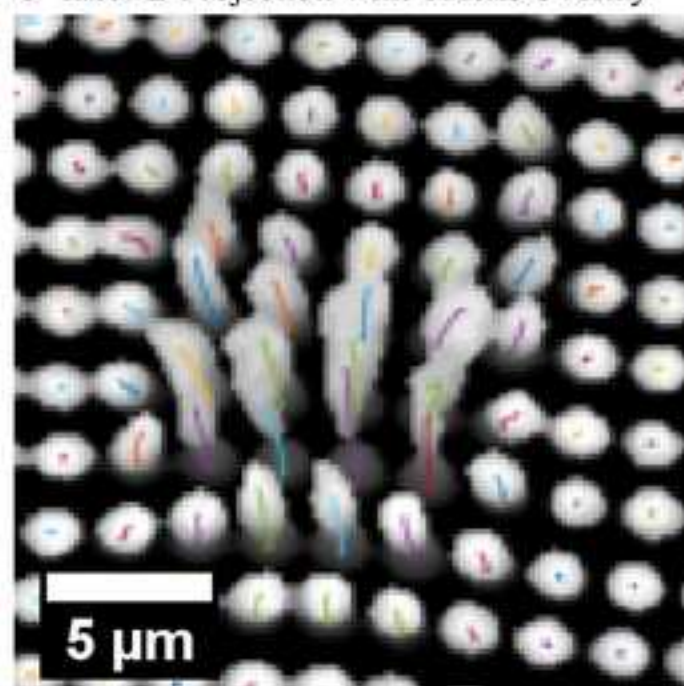
A Z-Projection of Fluorescent Markers



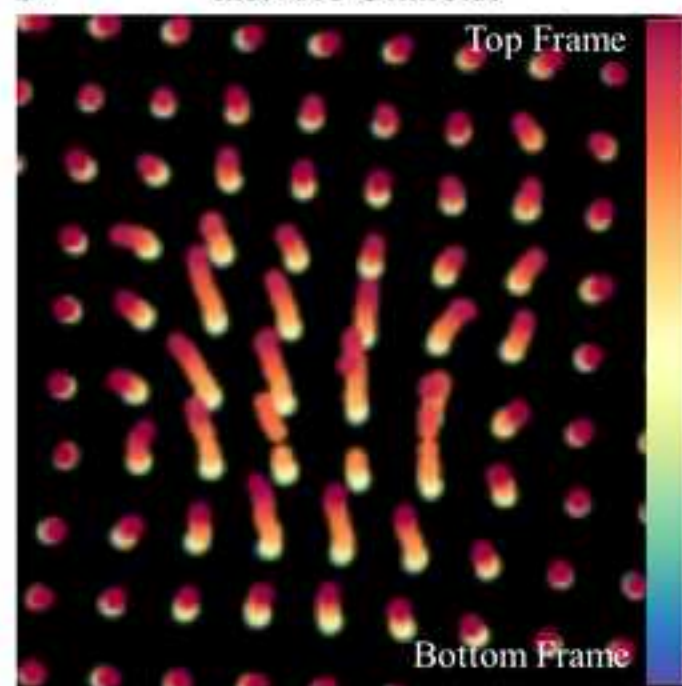
B Detected XY Centroids

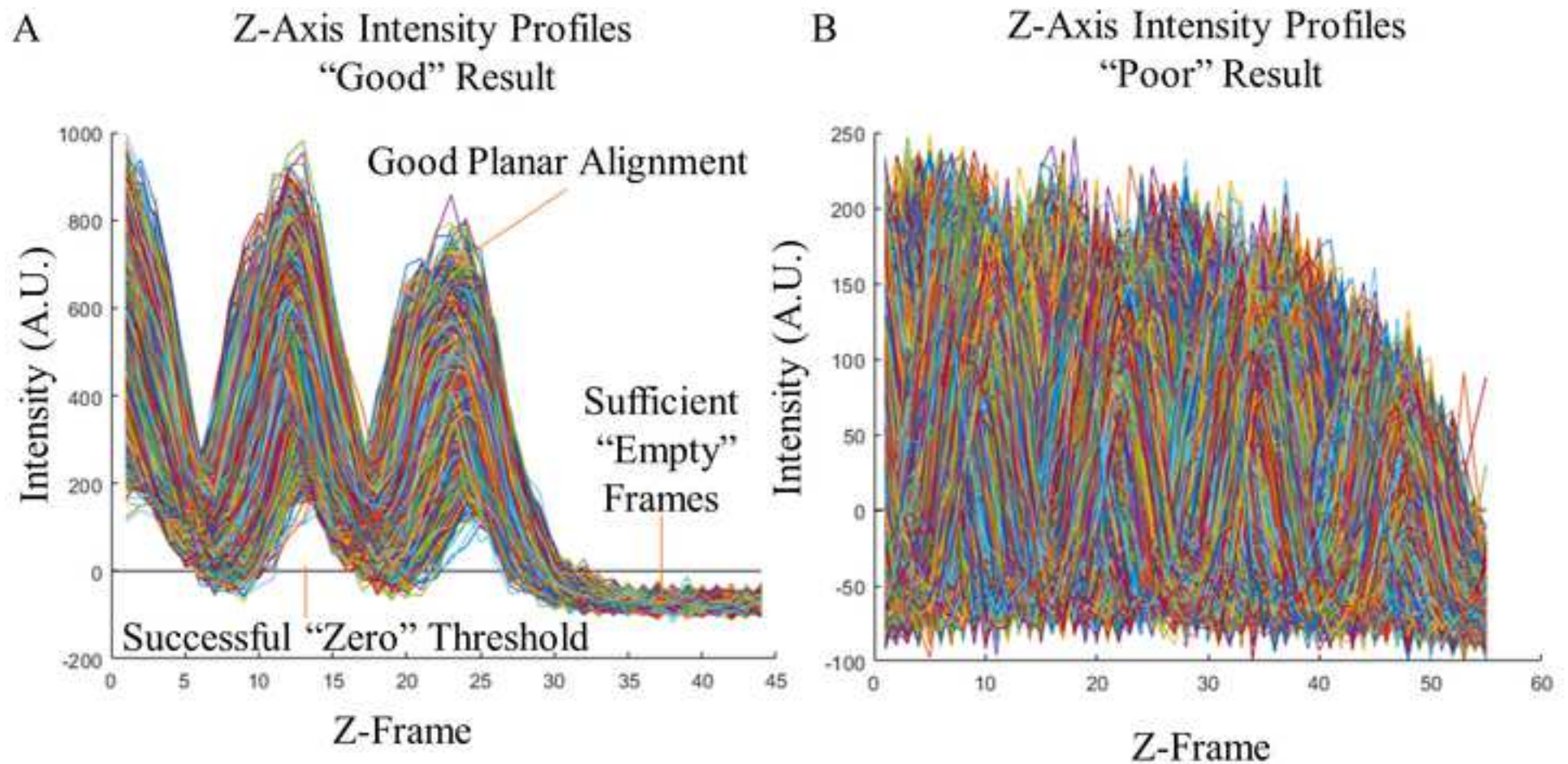


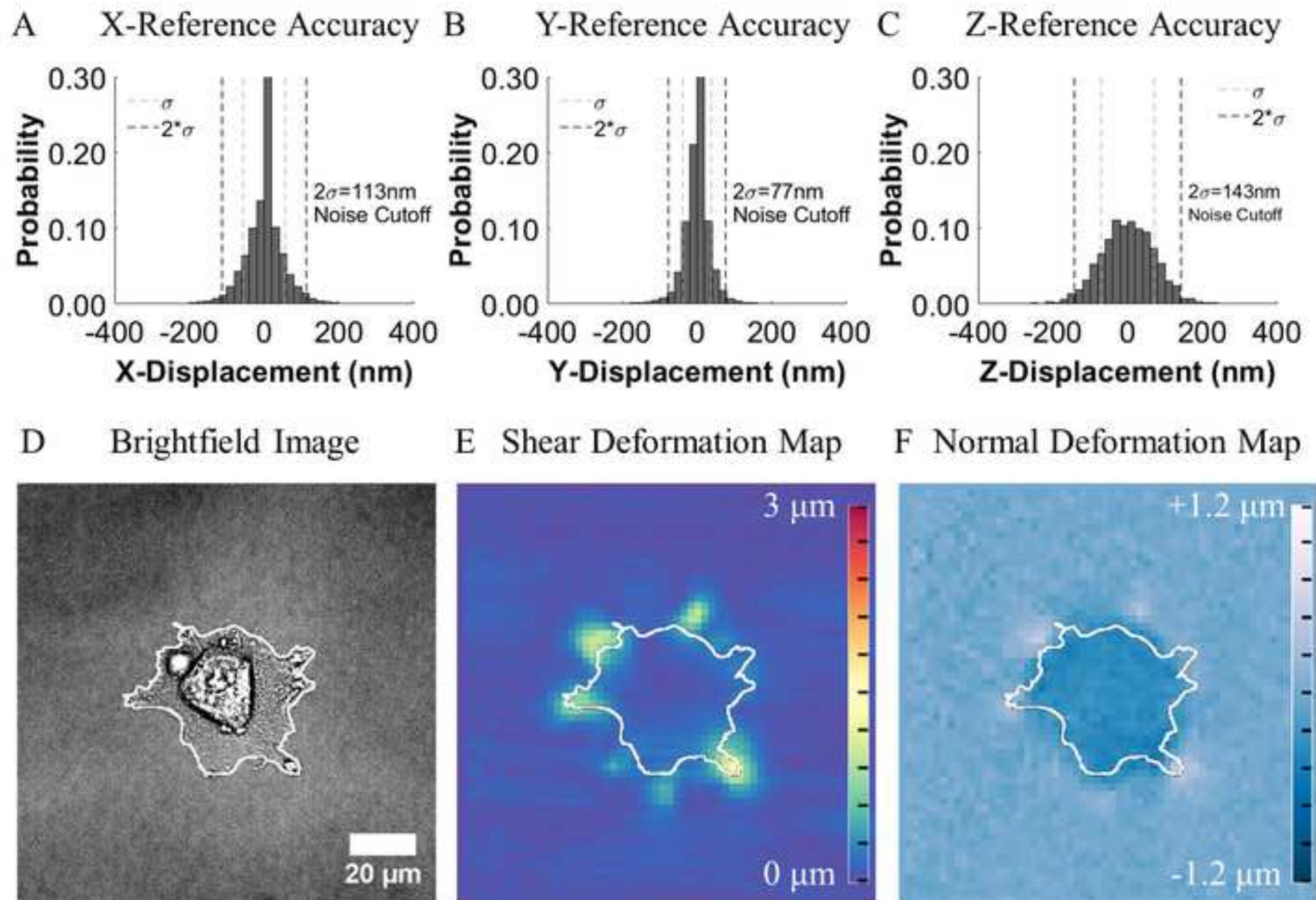
C Inset Z-Projection with Tracks Overlay

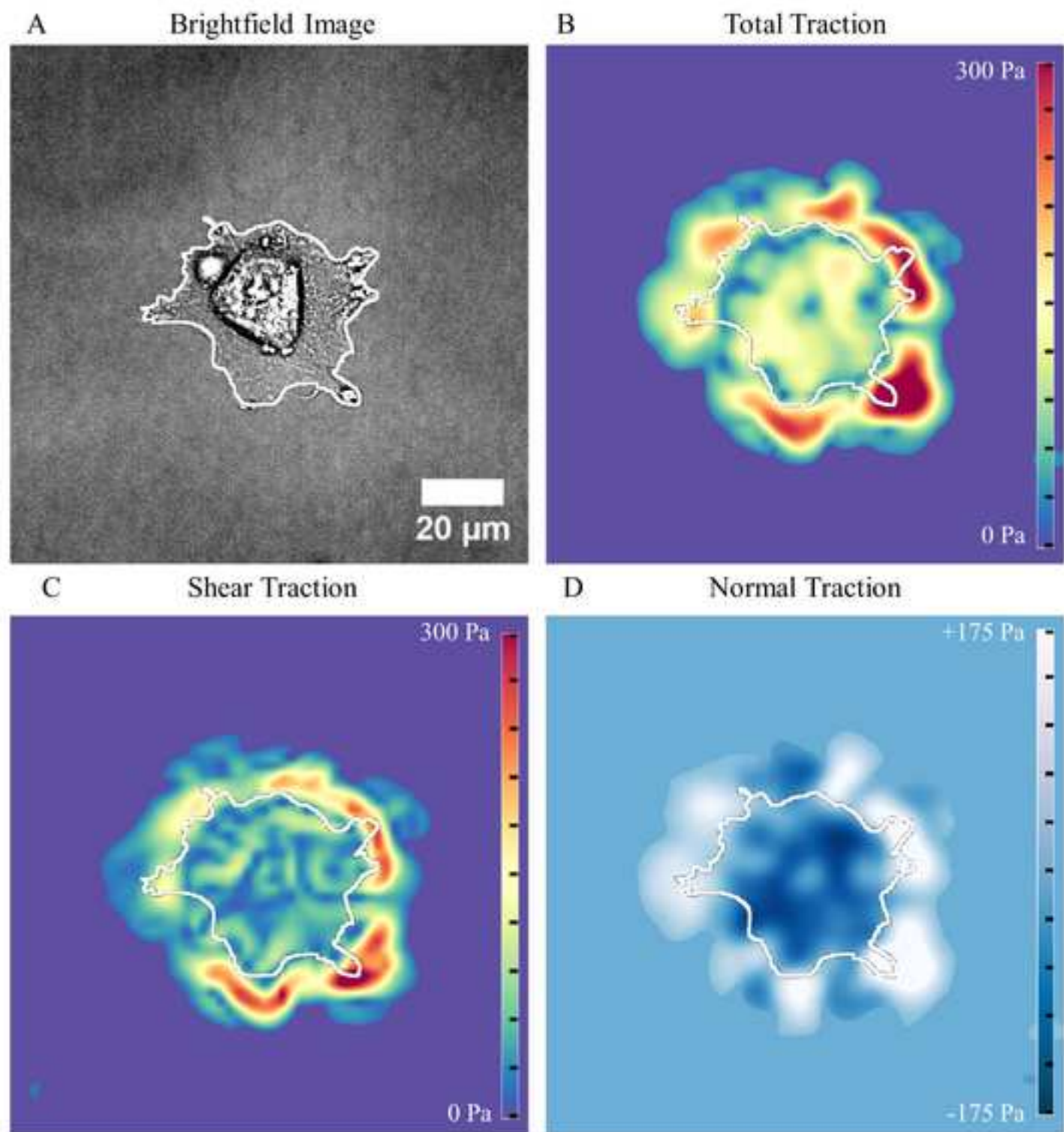


D Inset XY Centroids









Name of Material/ Equipment	Company	Catalog Number	Comments/Description
Acrodisc Syringe Filter, 0.2 µm Supor Membrane, Low Protein Binding Acrylate-Silane Functionalized #1.5 Coverslips	Pall	PN 4602	Allows for filtering of macromer solutions prior to base gel synthesis and subsequent lithography steps.
Axio-Observer Z1 w/Apotome	<i>in-house</i>	<i>in-house</i>	Acrylates allow binding of base hydrogel to the glass surface to immobilize the hydrogels. See reference: 21-24
Chameleon Vision ii	Zeiss		Widefield microscope with structured illumination module used to capture images for TFM.
Double Coated Tape, 9500PC, 6.0 mil	Coherent Inc.		Equipped on laser-scanning microscope used for multiphoton Lithography.
Flexmark90 PFW Liner	3M		Binds acrylate-silane functionalized coverslips to Petri dishes.
LSM-880	FLEXcon	FLX000620	Allows lining of double coated tape enabling feeding of tape into plotter.
MATLAB	Zeiss		Laser-Scanning microscope used for Multiphoton Lithography.
Model SC Plotter	Mathworks	R2018a	Runs custom scripts to generate lithography instructions for microscope and for analysis of TFM data.
Objective C-Apochromat 40x/1.20 W Corr M27	USCutter	SC631E	Cuts double coated tape into rings to bind coverslips to petri dishes.
PEG-AF633	Zeiss		Equipped on both widefield microscope and laser-scanning microscope to be used for both lithography and TFM.
PEG-DA	<i>in-house</i>	<i>in-house</i>	Fluorophore-labeled acrylate PEG variant for creating fiducial markers. See reference: 21
PEG-RGDS	<i>in-house</i>	<i>in-house</i>	Base material for hydrogels. See reference: 21
Petri Dishes	<i>in-house</i>	<i>in-house</i>	RGDS peptide-labeled mono-acrylate PEG variant for promoting cell-adhesion. See reference: 21
	CELLTREAT	229638	8mm holes are cut into the center of each dish using a coring bit to fit base hydrogels.

Sylgard 184 Silicone Elastomer Kit	Dow Corning	3097358-1004	For creating spacers to control base hydrogel thickness (aka PDMS).
Syringe, Leur-Lok, 1 mL	BD	309628	Allows for filtering of macromer solutions prior to base gel synthesis and subsequent lithography steps.
UV Lamp	UVP	Blak-Ray® B-100AP	Polymerizes base hydrogel.
1-vinyl-2-pyrrolidinone (NVP)	Sigma-Aldrich	V3409-5G	Radical accelerant and co-monomer. Improves pegylated fluorophore incorporation during lithography.



1 Alewife Center #200
Cambridge, MA 02140
tel. 617.945.9051
www.jove.com

ARTICLE AND VIDEO LICENSE AGREEMENT

Title of Article:	Fabrication and Implementation of a Reference-Free Traction Force Microscopy Platform
Author(s):	Omar Banda and John Slater

Item 1: The Author elects to have the Materials be made available (as described at <http://www.jove.com/publish>) via:

☒ Standard Access ☐ Open Access

Item 2: Please select one of the following items:

- ☒ The Author is **NOT** a United States government employee.
- ☐ The Author is a United States government employee and the Materials were prepared in the course of his or her duties as a United States government employee.
- ☐ The Author is a United States government employee but the Materials were NOT prepared in the course of his or her duties as a United States government employee.

ARTICLE AND VIDEO LICENSE AGREEMENT

1. **Defined Terms.** As used in this Article and Video License Agreement, the following terms shall have the following meanings: “**Agreement**” means this Article and Video License Agreement; “**Article**” means the article specified on the last page of this Agreement, including any associated materials such as texts, figures, tables, artwork, abstracts, or summaries contained therein; “**Author**” means the author who is a signatory to this Agreement; “**Collective Work**” means a work, such as a periodical issue, anthology or encyclopedia, in which the Materials in their entirety in unmodified form, along with a number of other contributions, constituting separate and independent works in themselves, are assembled into a collective whole; “**CRC License**” means the Creative Commons Attribution-Non Commercial-No Derivs 3.0 Unported Agreement, the terms and conditions of which can be found at: <http://creativecommons.org/licenses/by-nc-nd/3.0/legalcode>; “**Derivative Work**” means a work based upon the Materials or upon the Materials and other pre-existing works, such as a translation, musical arrangement, dramatization, fictionalization, motion picture version, sound recording, art reproduction, abridgment, condensation, or any other form in which the Materials may be recast, transformed, or adapted; “**Institution**” means the institution, listed on the last page of this Agreement, by which the Author was employed at the time of the creation of the Materials; “**JoVE**” means MyJoVE Corporation, a Massachusetts corporation and the publisher of The Journal of Visualized Experiments; “**Materials**” means the Article and / or the Video; “**Parties**” means the Author and JoVE; “**Video**” means any video(s) made by the Author, alone or in conjunction with any other parties, or by JoVE or its affiliates or agents, individually or in collaboration with the Author or any other parties, incorporating all or any portion

of the Article, and in which the Author may or may not appear.

2. **Background.** The Author, who is the author of the Article, in order to ensure the dissemination and protection of the Article, desires to have the JoVE publish the Article and create and transmit videos based on the Article. In furtherance of such goals, the Parties desire to memorialize in this Agreement the respective rights of each Party in and to the Article and the Video.

3. **Grant of Rights in Article.** In consideration of JoVE agreeing to publish the Article, the Author hereby grants to JoVE, subject to **Sections 4** and **7** below, the exclusive, royalty-free, perpetual (for the full term of copyright in the Article, including any extensions thereto) license (a) to publish, reproduce, distribute, display and store the Article in all forms, formats and media whether now known or hereafter developed (including without limitation in print, digital and electronic form) throughout the world, (b) to translate the Article into other languages, create adaptations, summaries or extracts of the Article or other Derivative Works (including, without limitation, the Video) or Collective Works based on all or any portion of the Article and exercise all of the rights set forth in (a) above in such translations, adaptations, summaries, extracts, Derivative Works or Collective Works and (c) to license others to do any or all of the above. The foregoing rights may be exercised in all media and formats, whether now known or hereafter devised, and include the right to make such modifications as are technically necessary to exercise the rights in other media and formats. If the “Open Access” box has been checked in **Item 1** above, JoVE and the Author hereby grant to the public all such rights in the Article as provided in, but subject to all limitations and requirements set forth in, the CRC License.

ARTICLE AND VIDEO LICENSE AGREEMENT

4. **Retention of Rights in Article.** Notwithstanding the exclusive license granted to JoVE in **Section 3** above, the Author shall, with respect to the Article, retain the non-exclusive right to use all or part of the Article for the non-commercial purpose of giving lectures, presentations or teaching classes, and to post a copy of the Article on the Institution's website or the Author's personal website, in each case provided that a link to the Article on the JoVE website is provided and notice of JoVE's copyright in the Article is included. All non-copyright intellectual property rights in and to the Article, such as patent rights, shall remain with the Author.

5. **Grant of Rights in Video – Standard Access.** This **Section 5** applies if the "Standard Access" box has been checked in **Item 1** above or if no box has been checked in **Item 1** above. In consideration of JoVE agreeing to produce, display or otherwise assist with the Video, the Author hereby acknowledges and agrees that, Subject to **Section 7** below, JoVE is and shall be the sole and exclusive owner of all rights of any nature, including, without limitation, all copyrights, in and to the Video. To the extent that, by law, the Author is deemed, now or at any time in the future, to have any rights of any nature in or to the Video, the Author hereby disclaims all such rights and transfers all such rights to JoVE.

6. **Grant of Rights in Video – Open Access.** This **Section 6** applies only if the "Open Access" box has been checked in **Item 1** above. In consideration of JoVE agreeing to produce, display or otherwise assist with the Video, the Author hereby grants to JoVE, subject to **Section 7** below, the exclusive, royalty-free, perpetual (for the full term of copyright in the Article, including any extensions thereto) license (a) to publish, reproduce, distribute, display and store the Video in all forms, formats and media whether now known or hereafter developed (including without limitation in print, digital and electronic form) throughout the world, (b) to translate the Video into other languages, create adaptations, summaries or extracts of the Video or other Derivative Works or Collective Works based on all or any portion of the Video and exercise all of the rights set forth in (a) above in such translations, adaptations, summaries, extracts, Derivative Works or Collective Works and (c) to license others to do any or all of the above. The foregoing rights may be exercised in all media and formats, whether now known or hereafter devised, and include the right to make such modifications as are technically necessary to exercise the rights in other media and formats. For any Video to which this **Section 6** is applicable, JoVE and the Author hereby grant to the public all such rights in the Video as provided in, but subject to all limitations and requirements set forth in, the CRC License.

7. **Government Employees.** If the Author is a United States government employee and the Article was prepared in the course of his or her duties as a United States government employee, as indicated in **Item 2** above, and any of the licenses or grants granted by the Author hereunder exceed the scope of the 17 U.S.C. 403, then the rights granted hereunder shall be limited to the maximum

rights permitted under such statute. In such case, all provisions contained herein that are not in conflict with such statute shall remain in full force and effect, and all provisions contained herein that do so conflict shall be deemed to be amended so as to provide to JoVE the maximum rights permissible within such statute.

8. **Protection of the Work.** The Author(s) authorize JoVE to take steps in the Author(s) name and on their behalf if JoVE believes some third party could be infringing or might infringe the copyright of either the Author's Article and/or Video.

9. **Likeness, Privacy, Personality.** The Author hereby grants JoVE the right to use the Author's name, voice, likeness, picture, photograph, image, biography and performance in any way, commercial or otherwise, in connection with the Materials and the sale, promotion and distribution thereof. The Author hereby waives any and all rights he or she may have, relating to his or her appearance in the Video or otherwise relating to the Materials, under all applicable privacy, likeness, personality or similar laws.

10. **Author Warranties.** The Author represents and warrants that the Article is original, that it has not been published, that the copyright interest is owned by the Author (or, if more than one author is listed at the beginning of this Agreement, by such authors collectively) and has not been assigned, licensed, or otherwise transferred to any other party. The Author represents and warrants that the author(s) listed at the top of this Agreement are the only authors of the Materials. If more than one author is listed at the top of this Agreement and if any such author has not entered into a separate Article and Video License Agreement with JoVE relating to the Materials, the Author represents and warrants that the Author has been authorized by each of the other such authors to execute this Agreement on his or her behalf and to bind him or her with respect to the terms of this Agreement as if each of them had been a party hereto as an Author. The Author warrants that the use, reproduction, distribution, public or private performance or display, and/or modification of all or any portion of the Materials does not and will not violate, infringe and/or misappropriate the patent, trademark, intellectual property or other rights of any third party. The Author represents and warrants that it has and will continue to comply with all government, institutional and other regulations, including, without limitation all institutional, laboratory, hospital, ethical, human and animal treatment, privacy, and all other rules, regulations, laws, procedures or guidelines, applicable to the Materials, and that all research involving human and animal subjects has been approved by the Author's relevant institutional review board.

11. **JoVE Discretion.** If the Author requests the assistance of JoVE in producing the Video in the Author's facility, the Author shall ensure that the presence of JoVE employees, agents or independent contractors is in accordance with the relevant regulations of the Author's institution. If more than one author is listed at the beginning of this Agreement, JoVE may, in its sole

ARTICLE AND VIDEO LICENSE AGREEMENT

discretion, elect not take any action with respect to the Article until such time as it has received complete, executed Article and Video License Agreements from each such author. JoVE reserves the right, in its absolute and sole discretion and without giving any reason therefore, to accept or decline any work submitted to JoVE. JoVE and its employees, agents and independent contractors shall have full, unfettered access to the facilities of the Author or of the Author's institution as necessary to make the Video, whether actually published or not. JoVE has sole discretion as to the method of making and publishing the Materials, including, without limitation, to all decisions regarding editing, lighting, filming, timing of publication, if any, length, quality, content and the like.

12. **Indemnification.** The Author agrees to indemnify JoVE and/or its successors and assigns from and against any and all claims, costs, and expenses, including attorney's fees, arising out of any breach of any warranty or other representations contained herein. The Author further agrees to indemnify and hold harmless JoVE from and against any and all claims, costs, and expenses, including attorney's fees, resulting from the breach by the Author of any representation or warranty contained herein or from allegations or instances of violation of intellectual property rights, damage to the Author's or the Author's institution's facilities, fraud, libel, defamation, research, equipment, experiments, property damage, personal injury, violations of institutional, laboratory, hospital, ethical, human and animal treatment, privacy or other rules, regulations, laws, procedures or guidelines, liabilities and other losses or damages related in any way to the submission of work to JoVE, making of videos by JoVE, or publication in JoVE or elsewhere by JoVE. The Author shall be responsible for, and shall hold JoVE harmless from, damages caused by lack of sterilization, lack of cleanliness or by contamination due to

the making of a video by JoVE its employees, agents or independent contractors. All sterilization, cleanliness or decontamination procedures shall be solely the responsibility of the Author and shall be undertaken at the Author's expense. All indemnifications provided herein shall include JoVE's attorney's fees and costs related to said losses or damages. Such indemnification and holding harmless shall include such losses or damages incurred by, or in connection with, acts or omissions of JoVE, its employees, agents or independent contractors.

13. **Fees.** To cover the cost incurred for publication, JoVE must receive payment before production and publication of the Materials. Payment is due in 21 days of invoice. Should the Materials not be published due to an editorial or production decision, these funds will be returned to the Author. Withdrawal by the Author of any submitted Materials after final peer review approval will result in a US\$1,200 fee to cover pre-production expenses incurred by JoVE. If payment is not received by the completion of filming, production and publication of the Materials will be suspended until payment is received.

14. **Transfer, Governing Law.** This Agreement may be assigned by JoVE and shall inure to the benefits of any of JoVE's successors and assignees. This Agreement shall be governed and construed by the internal laws of the Commonwealth of Massachusetts without giving effect to any conflict of law provision thereunder. This Agreement may be executed in counterparts, each of which shall be deemed an original, but all of which together shall be deemed to be one and the same agreement. A signed copy of this Agreement delivered by facsimile, e-mail or other means of electronic transmission shall be deemed to have the same legal effect as delivery of an original signed copy of this Agreement.

A signed copy of this document must be sent with all new submissions. Only one Agreement is required per submission.

CORRESPONDING AUTHOR

Name:

John Slater

Department:

Biomedical Engineering

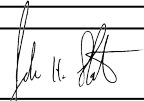
Institution:

University of Delaware

Title:

Assistant Professor

Signature:



Date:

06/03/2019

Please submit a **signed** and **dated** copy of this license by one of the following three methods:

1. Upload an electronic version on the JoVE submission site
2. Fax the document to +1.866.381.2236
3. Mail the document to JoVE / Attn: JoVE Editorial / 1 Alewife Center #200 / Cambridge, MA 02140

Editorial comments:

1. Please take this opportunity to thoroughly proofread the manuscript to ensure that there are no spelling or grammar issues.

The text was proofread and no spelling or grammar issues were identified.

2. The highlighted protocol steps are over the 2.75 page limit (including headings and spacing). Please highlight fewer steps for filming.

The amount of highlighted text has been reduced to 2.75 pages.

3. Step 4.1.2: Please write this step in the imperative tense.

This step has been combined with the subsequent step, which is in the imperative tense.

4. Step 5.1.2: Please write this step in the imperative tense.

The text in this step was edited into the imperative tense.

5. Step 6.1.3: Please write this step in the imperative tense.

The text in this step was edited into the imperative tense.

6. Please sort the items in alphabetical order according to the name of material/equipment.

The list had two items which began with numerical characters and were placed at the beginning of the list when sorted alphabetically using the sort function in excel. We assumed that these items were the issue referred to by this editorial request. For one item, the name was reorganized such that it no longer began with a numerical character and was then sorted alphabetically. For the other (1-vinyl-2-pyrrolidinone), the item was manually sorted to reflect beginning with the letter "v".